applied sciences

MDPI

Article

Face Image Inpainting of Tang Dynasty Female Terracotta Figurines Based on an Improved Global and Local Consistency Image Completion Algorithm

Qiangqiang Fan [1,*], Cong Wei [1], Shangyang Wu [2] and Jinhan Xie [1]

[1] College of Arts, Northeastern University, Shenyang 110819, China; 2410615@stu.neu.edu.cn (C.W.); 2101335@stu.neu.edu.cn (J.X.)
[2] College of Computer Science and Engineering, Northeastern University, Shenyang 110819, China; 2410838@stu.neu.edu.cn
* Correspondence: fanqq@mail.neu.edu.cn; Tel.: +86-13998830690

Featured Application: Image inpainting of Cultural Relics and Creation of Museum Cultural and Creative Products.

Abstract: Tang Dynasty female terracotta figurines, as important relics of ceramics art, have commonly suffered from natural and man-made damages, among which facial damage is severe. Image inpainting is widely used in cultural heritage fields such as murals and paintings, where rich datasets are available. However, its application in the restoration of Tang Dynasty terracotta figurines remains limited. This study first evaluates the extent of facial damage in Tang Dynasty female terracotta figurines, and then uses the Global and Local Consistency Image Completion (GLCIC) algorithm to restore the original appearance of female terracotta figurines, ensuring that the restored area is globally and locally consistent with the original image. To address the issues of scarce data and blurred facial features of the figurines, the study optimized the algorithm through data augmentation, guided filtering, and local enhancement techniques. The experimental results show that the improved algorithm has higher accuracy in restoring the shape features of the female figurines' faces, but there is still room for improvement in terms of color and texture features. This study provides a new technical path for the protection and inpainting of Tang Dynasty terracotta figurines, and proposes an effective strategy for image inpainting with data scarcity.

Keywords: Tang Dynasty female terracotta figurines; face image inpainting; global and local consistency image completion algorithm

check for updates

Citation: Fan, Q.; Wei, C.; Wu, S.; Xie, J. Face Image Inpainting of Tang Dynasty Female Terracotta Figurines Based on an Improved Global and Local Consistency Image Completion Algorithm. *Appl. Sci.* **2024**, *14*, 11621. https://doi.org/10.3390/app142411621

Academic Editor: Ion Sandu

Received: 29 October 2024
Revised: 10 December 2024
Accepted: 10 December 2024
Published: 12 December 2024

Copyright: © 2024 by the authors. Licensee MDPI, Basel, Switzerland. This article is an open access article distributed under the terms and conditions of the Creative Commons Attribution (CC BY) license (https://creativecommons.org/licenses/by/4.0/).

1. Introduction

Among the rich historical and cultural heritage of China, Tang Dynasty female terracotta figurines serve as important carriers of the social and artistic achievements of the Tang era. Their facial features are crucial for understanding the social landscape and aesthetic tastes of that time. However, due to natural erosion, human destruction, and other irresistible factors throughout history, many unearthed Tang Dynasty female terracotta figurines have suffered varying degrees of facial damage, such as the loss or damage of facial features. These damages not only affect the artistic expression of the artifacts, but also weaken their function as historical witnesses. Therefore, the precise image inpainting of these damaged Tang Dynasty female terracotta figurines is not only an urgent preservation task, but also an important means of protecting and inheriting Tang Dynasty cultural heritage.

Currently, common inpainting techniques can be divided into physical inpainting and digital inpainting. Digital inpainting includes two-dimensional image inpainting and three-dimensional virtual inpainting. During physical inpainting, the detailed

operations performed by experts may lead to the loss of original information, and may even cause further damage to the artifact itself. Three-dimensional virtual inpainting requires a vast amount of data and relies on the tight integration of multiple technical tools and processes. In contrast, image inpainting techniques exhibit significant advantages in terms of safety, accuracy, and convenience. As a result, in the field of cultural heritage inpainting, image inpainting techniques are gradually becoming the focus of research and application. Image inpainting is a technique that allows for filling missing areas with appropriate content [1], effectively restoring and protecting artifacts without compromising their physical integrity. Moreover, it enables an in-depth study and widespread dissemination of artifacts' original states in a virtual environment, achieving long-term preservation and educational outreach for cultural heritage. Image inpainting algorithms can be mainly divided into traditional algorithms, optical methods, and machine learning-based algorithms. Traditional algorithms [2,3] are primarily classified into diffusion-based, exemplar-based, and sparse model-based methods. These approaches are suitable for completing images with similar structures in the surrounding background but have limitations when dealing with complex objects such as faces. Optical methods involve spectral imaging analysis, utilizing multispectral or hyperspectral data for cultural heritage image restoration. This technique captures spectral information across multiple bands, providing more details and information than traditional imaging, and has been widely applied in cultural heritage conservation [4–6]. However, spectral imaging generates large datasets, requiring significant computational resources for processing and storage. Machine learning-based image inpainting methods include support vector machines [7], nearest neighbor algorithms [8], clustering algorithms [9], Bayesian methods [10], random forests [10], generative adversarial networks (GANs) [11], and convolutional neural networks (CNNs) [12,13]. Traditional machine learning algorithms are suitable for small-scale repairs with minor damage, but are less effective in handling complex image structures. The introduction of deep learning [14,15], especially the application of GANs and CNNs, has brought revolutionary progress to the field of image inpainting. For instance, Yang et al. proposed a multi-scale neural patch synthesis method based on the joint optimization of image content and texture constraints, significantly enhancing high-resolution image restoration performance [16]. Compared to the encoder–decoder structure based on CNNs, the GAN structure adds a discriminator, which more effectively learns the distribution of real samples [15]. GAN-based algorithms, due to their powerful image generation capabilities, have been widely applied in the practice of cultural heritage image inpainting [11,17,18]. Face image inpainting, as a branch of image inpainting, leverages the semantic information of the entire face image to repair damage caused by occlusion or loss or reconstructs the entire face from the extracted semantic features. Currently, deep learning-based face image inpainting methods demonstrate the best performance. Although many methods combine GANs with various prior knowledge techniques, their robustness still has room for improvement.

Currently, in the field of cultural heritage with rich datasets, such as murals and paintings, image inpainting has achieved significant accomplishments [4,13,19–21]. However, in the field of ceramic image inpainting, related research is relatively scarce, mainly due to the lack of available data. Compared to the mural and painting fields, where datasets typically contain thousands of well-preserved images, the datasets in the ceramic field only consist of a few hundred complete images. Therefore, in the restoration of ceramic, some studies use daily ceramic with similar shapes as substitute data for archaeological ceramic [22], while other studies use traditional restoration methods that do not rely on large amounts of data. Ref. [23] proposed an automated pattern completion method based on rule reasoning for the repetitive surface patterns commonly found in ancient ceramics. This method relies on known pattern sequence information rather than the data-driven strategies of deep learning, making it more suitable for completing images with low-level semantic information. However, it is challenging to effectively restore images containing

high-level semantic information, such as facial features. In the research field of Tang Dynasty ceramics, current work mainly focuses on 3D-shape inpainting [24,25], and image inpainting technology has not yet been applied.

The Global and Local Consistency Image Completion (GLCIC) algorithm, based on convolutional neural networks, is a classic algorithm that has shown significant advantages in the field of image restoration. By combining multi-scale convolutional networks, it ensures the coordination of the overall structure and local details in the restored images, demonstrating great potential for image restoration in data-scarce situations. This study reveals that most of the facial images of Tang Dynasty female terracotta figurines exhibit moderate defects, primarily local. Consequently, during the restoration process, it is crucial to ensure the coordination and integrity between local details and the overall structure. Based on this, we reasonably infer that this method has a high probability of successfully restoring the facial images of Tang Dynasty female terracotta figurines, even when data are scarce. However, currently, there is no specifically designed algorithm for completing the facial images of Tang Dynasty female figurines; a dataset of Tang Dynasty terracotta figurines based on the GLCIC algorithm has not yet been constructed; and most importantly, the effectiveness of GLCIC in restoring the facial images of Tang Dynasty female figurines remains unknown.

To address the aforementioned challenges, the goal of this study was to optimize the GLCIC algorithm to achieve the precise inpainting of damaged faces using the limited available data, thereby improving the accuracy and quality of the inpainting, and to provide more accurate reference samples for the restoration of Tang Dynasty female ceramic figurines, as well as to offer reference solutions for the material selection of figurines from the same era. The structure of this paper is arranged as follows. First, we will review the relevant literature and research background to lay the theoretical foundation for this study. Next, we will detail the design and implementation of our method, including the initial assessment of the extent of facial damage in Tang Dynasty figurines, comparison of facial image restoration algorithms, and the final implementation of facial image restoration for Tang figurines. Subsequently, we will present experimental results and conduct an analysis and discussion. Finally, we will summarize our research findings. This study compiled and constructed a dataset of Tang Dynasty terracotta figurines and incorporated three modules into the Global and Local Consistency Image Completion (GLCIC) algorithm: a data augmentation module, a guided filtering module, and a local enhancement module. These enhancements enable the fine restoration of facial details, providing a new technological pathway for the protection and restoration of Tang Dynasty ceramic heritage. Additionally, this study expands the application scope of the GLCIC algorithm and proposes effective strategies for image restoration under data-scarce conditions.

2. Historical Background

2.1. Tang Dynasty Female Terracotta Figurines

Terracotta figurines are ancient burial sculptures, typically made of clay and fired. The art of figurines in ancient China began to develop during the Spring and Autumn and Warring States periods, reaching its peak through the Qin, Han, Northern and Southern Dynasties, and Sui, culminating in the Tang Dynasty. The main achievements of Tang figurines lie in their creation of various forms that vividly reflect real life, possessing high aesthetic and historical value. The sculpting techniques of Tang Dynasty figurines were advanced, with accurate proportions of body parts and overall harmony. Both male and female terracotta figurines were intricately detailed and lifelike [26]. Tang Dynasty female terracotta figurines are diverse, including noblewomen figurines, maid figurines, horse-riding figurines, and music and dance figurines, among others [27]. These figurines were crafted to reflect different genders, statuses, and personalities.

In terms of decoration methods, Tang Dynasty figurines can be categorized into painted figurines, painted glazed figurines, and multicolored glazed figurines [28]. Painted figurines are made of clay, fired, and then coated with a layer of white material called

makeup clay or white clay powder. The surface is then painted and rendered with colors as needed. Painted glazed figurines are painted on a single glaze color, combining painting and glazing. Multicolored glazed figurines typically feature green, brown, and white or green, yellow, and white glazes, commonly known as "Tang Tri-Color Glazed Ceramics" [27]. Tang Tri-Color Glazed Ceramics often uses a combination of glaze and paint. To enhance the texture of the figurines, the faces of the figurines were left unglazed. After firing, the heads were coated with white powder, the lips painted red, and the pupils, eyebrows, beards, and shoes painted black. This technique is known as "Kaixiang" (facial painting technique). The use of the "Kaixiang" technique significantly enhanced the realism and vividness of the Tang Tri-Color Glazed figurines in artistic expression [29].

The development and changes in the art of Tang Dynasty figurines can be divided into three periods: early, middle, and late. During the early Tang period, women held a relatively high status and exhibited open behavior, often appearing in public for entertainment activities such as horseback riding, which was a popular trend [30]. The female terracotta figurines of horse riders from the tomb of Zheng Rentai are representative works of this period. These figurines typically feature wide eyebrows, red lips, large eyes, gentle facial expressions, and dignified demeanors. The faces of early Tang female terracotta figurines are usually delicate, with peaceful expressions, slender bodies, and tight-fitting clothing that accentuates their graceful figures. In the middle Tang period, Tang figurines fully shed the transitional characteristics of early Tang figurines, displaying a mature era style that embodies the unique, splendid, and vigorous aesthetic features of Tang art [31]. Female terracotta figurines from this period have plump faces, soft necks, and minimal dynamic poses. Both the facial expressions and the overall structure of the figurines exude a serene atmosphere. Many women of this time liked to apply red blush on their cheeks, a makeup technique known as "drunken blush makeup", which was very popular. These young women, with elegant and dignified postures, often wore gentle smiles [32]. During the late Tang period, female terracotta figurines became increasingly prominent in the art of terracotta figurines, with more refined and exquisite craftsmanship compared to other periods. The late Tang female terracotta figurines evolved from the full and voluminous female terracotta images formed in the middle period, featuring fuller and more substantial bodies, with more realistic and delicate facial expressions. The demeanor of these female terracotta figurines generally conveyed a sense of calm and serenity [30].

The artistic style of Tang Dynasty female terracotta figurines varied across different periods, reflecting the changes in social customs and aesthetic trends of the time. However, their facial features remained consistently distinctive. The facial features of Tang Dynasty female terracotta figurines are generally characterized by delicate and concentrated features, presenting a beautiful visage (Figure 1). They have slender eyes with upturned corners, thin curved eyebrows, small cherry-like mouths, and smiles that are subtle yet expressive [33]. For example, the painted female terracotta figurines with loose hair unearthed from Tang tombs in Gongyi have clear and beautiful eyebrows, high-arched brows, slender eyes, high noses, red lips, floral decorations on their foreheads, and red blush on their cheeks. Their hair, eyebrows, and skirt folds are painted in black [34]. The painted female terracotta figurines in the Xi'an Museum have faces painted with red powder, silkworm-like eyebrows, and facial features that are relatively concentrated in the center of the face, appearing slightly compact. The male-dressed female terracotta figurines in the Shaanxi Tang Tri-Color Glazed Ceramics Museum, although dressed in male attire, exhibit a graceful and feminine posture, with thin eyebrows, small eyes, red lips, and a charming appearance (Figure 2). Through the review of the above literature, it can be seen that Tang Dynasty female terracotta figurines possess a strong artistic style with distinct facial features and consistent facial painting methods. Therefore, the faces of Tang Dynasty female terracotta figurines are suitable for inpainting using deep learning techniques.



(**a**) (**b**) (**c**)

Figure 1. (**a**) Painted terracotta female figurine; (**b**) standing terracotta female figurine; (**c**) seated terracotta female figurine with a tricolor phoenix crown and bird (Source: the Palace Museum).



Figure 2. Tang Dynasty male-dressed female terracotta figurine (Source: Shaanxi History Museum).

2.2. Image Inpainting of Cultural Heritage

Image inpainting is a technique that allows for filling in missing areas with appropriate content, aiming to predict the missing regions from a single damaged image [1], i.e., two-dimensional image inpainting. It has many applications in image editing, such as occlusion removal and the inpainting of old photographs. In the current research field, image inpainting work for cultural heritage mainly focuses on murals, ancient paintings, and other types of cultural heritage with relatively clear and abundant data [4,13,19–21].

Image inpainting algorithms can be divided into three categories: traditional algorithms, optical methods, and machine learning-based image inpainting algorithms. Additionally, these three methods can be combined to leverage their respective advantages, achieving more efficient image inpainting results. Traditional algorithms mainly rely on data similarity, with their core being texture generation or patch-matching techniques. They are based on the assumption that the missing parts should be restored by selecting similar textures or patches from known regions. Traditional algorithms can be simply divided into

three categories: diffusion-based methods [35], exemplar-based methods [36], and sparse model-based methods [37] for image inpainting [3,4]. Regarding diffusion-based methods, ref. [38] proposed a diffusion probability model that reconstructs high-definition images of traditional Chinese landscape paintings through an iterative denoising process. Regarding exemplar-based methods, Ref. [2] proposed a classic inpainting method that removes a large object based on the calculation of patch priority and similarity while preserving important texture and structural information. Many papers have improved the Criminisi algorithm to achieve image inpainting for cultural heritage [17]. Ref. [39] used an improved Criminisi algorithm based on structure tensors to restore damaged images of ancient fabrics, showing that the algorithm results in more reasonable texture structures and fewer inpainting traces. Ref. [40] proposed a structure-guided virtual inpainting method based on the Criminisi algorithm, reconstructing missing structural lines of silk artifacts through adaptive curve fitting and optimizing the inpainting priority and sample block size selection mechanism to improve the inpainting effect. Regarding sparse model-based methods, Ref. [41] proposed a line-drawing-guided mural inpainting method that addresses the digital restoration of Dunhuang murals by sparsely modeling texture similarity and structure continuity. Traditional algorithms perform well in background inpainting tasks and are widely deployed in practical applications. However, because they assume that the missing patches can be found somewhere in the background area, if there is not enough similar structural information near the missing area or if the image itself is complex and irregular (such as faces or objects), structure-guided virtual inpainting methods may face challenges, as they rely on known information to infer and reconstruct the missing parts [42].

Spectral imaging technology also plays an important role in the field of cultural heritage image restoration [4–6]. This technology combines image capture and the analysis of an object's spectral reflectance, allowing for the characterization of the object's features across multiple bands. Spectral imaging analysis includes ultispectral imaging, hyperspectral imaging, and Fourier transform spectral imaging. Ref. [43] proposed a new method based on a multispectral imaging system, using infrared spectral information to separate and restore degraded areas in the visible spectrum, thereby improving the visual quality of degraded historical document images. Ref. [4] proposed an automated system based on hyperspectral imaging for extracting and restoring scratches on the mural on the east wall of Cave 6 at Yungang Grottoes. The authors combined spectral imaging analysis with traditional algorithms, enhancing information through principal component analysis (PCA) and high-pass filtering, using multi-scale top-hat transformation, Otsu's segmentation, connected component analysis, and dilation operations to extract scratch information, and performing virtual restoration through an improved exemplar-based region filling method. The main drawbacks of spectral imaging analysis are its high equipment costs and the extremely large amount of data it generates, which require significant computational resources for processing and storage. It is also more effective at detecting minor damages but less effective for large-scale damage.

Currently, machine learning-based image inpainting algorithms, ranging from basic statistical methods like linear regression to complex deep learning models, have been widely applied in the field of cultural heritage restoration, including support vector machines [7], nearest neighbor algorithms [8], clustering algorithms [9], Bayesian methods [10], random forests [10], GANs [11], and CNNs [12,13]. Many traditional machine learning algorithms are combined with traditional methods for image inpainting. Ref. [9] proposed digitally enhancing and restoring degraded mural images through weighted averaging of the original image and mean image, combined with line detection, K-means clustering, pixel averaging, and weighted averaging steps. Ref. [44] proposed a method that combines global and local feature weighting, performing virtual restoration of ancient murals based on structure guidance, using elastic net regularization-sparse representation model and neighborhood similarity estimation to enhance the consistency of global and local features in mural restoration. However, these methods still suffer from the same drawbacks as traditional algorithms mentioned above.

Regarding deep learning-based image inpainting methods, they currently offer the best performance and effectiveness in the field of cultural heritage image restoration. These methods excel in restoring complex image structures by learning extensive information from large datasets and typically treat image inpainting as a conditional image generation problem [45], where known pixels are considered as conditions. Ref. [12] proposed the Coherent Semantic Attention (CSA) algorithm, which uses an attention mechanism to find similar regions and utilizes the surrounding areas' similar semantic information to restore the image. Although this method increases the difficulty and time of training, it better preserves the contextual structure of the image. Ref. [18] proposed the SeparaFill method, based on GANs and U-Net, which divides the mural image restoration process into two steps: contour inpainting and content filling. The results show that this method outperforms existing techniques in terms of the restoration effect and detail preservation. Ref. [11] proposed a Sketch-Guided Restoration Generative Adversarial Network (SGR-GAN) framework for restoring Chinese landscape paintings, resulting in images that better match human visual perception. Ref. [13] proposed a GAN model for restoring Dunhuang mural images, improving the restoration effect through parallel dual convolution and ternary discriminators. Ref. [46] proposed an image inpainting method based on U-Net, MobileNet, and Pix2pix for restoring the colored paintings on weathered beams in the Forbidden City, dividing the paintings into three parts: background, golden edges, and dragon patterns, to be restored separately. The results showed good color and detail restoration. However, deep learning methods rely on a large number of samples as references to train models and extract image features. In large-area image inpainting, these methods may face challenges of insufficient inpainting and texture inconsistency [18]. Some studies have attempted to use small datasets for cultural heritage image inpainting and have achieved certain results, but the inpainting effect still faces challenges when dealing with facial images in murals [47].

2.3. Face Image Inpainting

Face image inpainting, also known as face restoration, aims to fill in the missing parts of a face using visually plausible predictions [48]. Face image inpainting is still under-researched and remains a challenging problem. Early inpainting works [49,50] involved copying suitable pixels or textures into the areas to be restored, relying on existing pixels to reconstruct the missing parts of the image. These methods are mainly suitable for images with only small areas of damage, and their inpainting effect depends on the existing pixel information within the image. Although there have been attempts to use improved diffusion-based inpainting algorithms [51] that do not rely on large datasets and long training times, they have not yet been widely applied and validated. Some methods based on deep learning [14,15,52,53] can directly predict the pixel values of the missing regions, generating high-quality results for the missing areas. Ref. [47] proposed STNet, which effectively restores missing regions by separately reconstructing the structural and textural information of the image and then merging them. It attempted to restore faces in murals with minimal data but failed to successfully reconstruct facial detail features. To further improve the quality of face image inpainting, many methods have adopted techniques that combine GANs with various prior knowledge. This prior knowledge includes facial parsing [54], facial landmark recognition [55], identity information priors [56], and 3D deformable models [57,58]. However, these methods face robustness issues when dealing with faces that have large pose variations and extensive damage, as they require additional networks to perform auxiliary tasks [59].

3. Materials and Methods

3.1. Research Design

The study aimed to provide a tool for modeling the missing parts of the figurines, and the research process is divided into the following three stages (Figure 3):

(1) Evaluation of Facial Deficiency in Tang Dynasty Female Terracotta Figurines: This stage employs the Fuzzy Analytic Hierarchy Process (FAHP) to systematically assess the degree of facial deficiency in Tang Dynasty female terracotta figurines.
(2) Comparison of Face-Image-Inpainting Algorithms: In this stage, the study applies the GLCIC algorithm and an improved GLCIC algorithm to restore the facial images of Tang Dynasty female terracotta figurines and compares the results. The effectiveness of the two algorithms is quantitatively compared using two objective evaluation indicators: the structural similarity index (SSIM) and the peak signal-to-noise ratio (PSNR).
(3) Inpainting and Evaluation of Tang Dynasty Female Terracotta Figurine Facial Images: Based on the results of the algorithm comparison, the improved GLCIC algorithm, which shows superior performance, is selected to finely restore the missing parts of the Tang Dynasty female terracotta figurines' faces. This stage focuses on the adaptive handling of the algorithm in practical applications Additionally, an Absolute Category Rating (ACR) was used to subjectively evaluate the restored faces of the Tang Dynasty female terracotta figurines. Finally, Pearson correlation analysis is conducted to explore the relationships between the evaluation metrics.

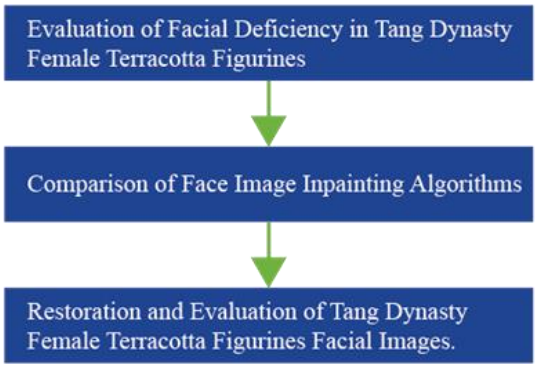


Figure 3. Research flowchart.

Through these three stages of research, this study aimed to provide a scientific and effective methodology for inpainting the missing parts of Tang Dynasty female terracotta figurines' faces and to conduct a multi-angle, multi-level evaluation of the inpainting effects.

3.2. Sample

The data used in the experiment were sourced from websites of the Shaanxi History Museum, the Palace Museum, the Metropolitan Museum of Art in New York, and the Shanghai Museum. This study collected a total of 891 photos, of which 45% of the Tang Dynasty figurines' faces were relatively intact. Consequently, 400 photos with complete faces of Tang Dynasty figurines were used as the training dataset. Some of the data are shown in Figure 4. Tang Dynasty female terracotta figurines are the most exquisitely depicted and representative category, and their quantity is relatively larger compared to other types of figurines. The main Tang Dynasty female terracotta figurines captured in this study include noblewomen figurines, maidservant figurines, and musical and dancing figurines. The facial features of these female terracotta figurines in the images are quite distinct: slender eyes, thin curved eyebrows, small cherry-like mouths, and concentrated facial features. In terms of decoration methods, these terracotta figurines include painted terracotta figurines, painted glazed terracotta figurines, and multicolored glazed terracotta figurines. The facial features of the female terracotta figurines, such as the lips, are painted red, while the pupils and eyebrows are painted black. These facial features fully reflect the aesthetic concepts and cultural characteristics of the Tang Dynasty.



(a) (b) (c) (d)

Figure 4. (**a**) Tricolor hand-in-hand standing female figurine; (**b**) painted terracotta standing female figurine; (**c**) tricolor horse-riding figurine; (**d**) tricolor hand-in-hand standing female figurine (Source: the Palace Museum).

3.3. Experimental Environment

This experiment was implemented using tools such as Torch and OpenCV. The software and support platforms required for the experiment are shown in Table 1.

Table 1. Software and support platforms required for the experiment.

Software/Support Platform	Version
Pycharm	PyCharm Community Edition 2021.3.2
Python	3.7
Windows	11
GPU	NVIDIA GeForce RTX 4060 Ti
CPU	Intel(R) Core (TM) i5-14400F

3.4. Facial Deficiency Evaluation

In this study, we conducted a preliminary analysis of the collected facial images of Tang Dynasty terracotta figurines and found that 55% of the samples had varying degrees of damage. To systematically evaluate the extent of this damage, we employed the Fuzzy Analytic Hierarchy Process (FAHP) to determine the importance of facial features of the figurines, followed by identifying the importance of image visual features. Finally, we derived the overall facial damage extent based on the weights and damage degrees of both aspects.

The FAHP method expands upon Saaty's Analytic Hierarchy Process (AHP) by incorporating the fuzzy set theory [60]. The fuzzy set theory, proposed by [61], introduces the concept of degrees to extend classical Boolean logic and set theory, allowing for conditions to be more flexible and capable of handling imprecision and uncertainty. Compared to traditional AHP, FAHP is more suitable for dealing with uncertainty and fuzzy information in decision-making [62,63]. Currently, FAHP has been widely applied in heritage field assessments [64]. The FAHP process in this study includes the following steps: (1) Define the top-level goal; (2) establish a hierarchical structure for the goal; (3) construct fuzzy judgment matrices and fuzzy weight vectors; (4) rank all alternatives and select the best one. We invited five experts in cultural heritage from Liaoning Museum and the Art College of Northeastern University to perform subjective evaluations and scoring. The study used the fuzzy linguistic variable set mentioned by [65] to score, ultimately determining the relative weights of multiple criteria and evaluating the reliability of these weights through consistency testing.

The human face is defined by its parts (such as eyes, nose, and mouth) and the spatial relationships between these parts and their subparts. Therefore, listing these parts is important. This study referred to the hierarchical framework in [66] and made appropriate adjustments based on the facial images of the figurines. The first top-level goal of the study

was to assess the importance of the facial features of the figurines, evaluating four aspects: eyes, eyebrows, nose, and mouth. Table 2 defines the 23 sub-criteria used to describe these four basic aspects.

Table 2. Evaluation criteria for the facial features of Tang Dynasty terracotta figurines.

Criteria	Sub-Criteria 1	Sub-Criteria 2	Sub-Criteria 3	Sub-Criteria 4	Sub-Criteria 5	Sub-Criteria 6	Sub-Criteria 7
Eyes	Shape of the lower eyelid	Distance between eyelids	Fissure length	Direction of the fissures	Inter-eye distance	Color	
Eyebrows	Length	Direction	Distance between the eyebrows	Position	Shape	Thickness	Color
Nose	Length	Width	Width of the nasal bridge	Shape of the nasal bridge	Shape of the nasal tip	Nostrils	
Mouth	Shape of the opening between lips	Fullness	Width	Width of the philtrum			

The second top-level goal of this study was to evaluate the importance of the visual features of Tang Dynasty female terracotta figurine facial images. The study evaluated these features from three aspects: color, texture, and shape. Table 3 defines the 11 sub-criteria used to describe these three basic aspects. The most common visual features of images include color, texture, and shape. Most image annotation and retrieval systems are built based on these features. Color features are described and quantified through parameters in specific color spaces (such as RGB, CMYK, HSV, etc.). In this study, we referred to the HSV color space and categorized color features into the following: hue (type of color), saturation (purity of color), and value (brightness of color) [67]. Texture features are the quantitative characteristics of the surface feel represented by visual patterns that are uniformly distributed in the image. Texture features can be divided into the following: coarseness (the granularity of the texture pattern), contrast (the difference between light and dark areas in the texture pattern), directionality (the directional distribution of the texture pattern), line-likeness (whether the texture pattern contains line-like structures), regularity (the regularity and repetitiveness of the texture pattern), and roughness (similar to coarseness but more focused on the tactile sense of the surface) [68]. Shape features are used to identify and encode the geometric characteristics of real-world objects and can be analyzed through contours or regions. Contour features describe the shape through the boundaries of the object, while region features describe the characteristics within the shape [67].

Table 3. Evaluation criteria for image visual features.

Criteria	Sub-Criteria 1	Sub-Criteria 2	Sub-Criteria 3	Sub-Criteria 4	Sub-Criteria 5	Sub-Criteria 6
Color	Hue	Saturation	Value			
Texture	Coarseness	Contrast	Directionality	Line-likeness	Regularity	Roughness
Shape	Contour Features	Regional Features				

After calculating the weights, the authors evaluated the extent of facial damage in the Tang Dynasty female terracotta figurines using Formula (1). Here, S_j is the damage extent of the facial feature i, W_i is the weight of the facial feature i, W_j is the weight of the visual feature j within the facial feature i, and S_{ij} is the damage extent of the visual feature j within the facial feature i. S_T represents the overall facial damage extent of the figurines.

$$S_T = \sum_i W_i \times \left(\sum_j W_j \times S_{ij} \right) \quad (1)$$

3.5. Face Image Completion

3.5.1. GLCIC Algorithm

The Global and Local Consistent Image Completion (GLCIC) algorithm is a deep convolutional neural network-based algorithm specifically designed for image completion tasks [14]. This algorithm consists of three neural networks: a completion network and two context discriminator networks. The completion network is used for image completion, while the two context discriminator networks, namely the global and local discriminators, are used to train the completion network to achieve realistic image completion. The global discriminator network takes the entire image as input, whereas the local discriminator network only takes a small region around the completion area as input. Both discriminator networks are trained to determine whether an image is real or completed by the completion network, while the completion network is trained to deceive these two discriminator networks. Only by jointly training these three networks can the completion network achieve the realistic completion of diverse images. Unlike other methods that focus on image generation, this method does not generate images from noise, which helps stabilize the initial training process.

However, the GLCIC algorithm encountered several challenges while restoring the facial features of the Tang Dynasty terracotta figurines. Firstly, the number of existing Tang figurines is limited, making it difficult to support the large data requirements needed for training. Secondly, due to the erosion of time, most Tang female terracotta figurines' faces are mottled and damaged, with the main facial features generally missing or incomplete. Lastly, due to the characteristics of the completion network, the image completion is based on regional features, which can result in the smoothing of features with the surrounding area after completing the facial features of Tang female terracotta figurines, as shown in Figure 5. Figures 5 and 6 below show the results of training and restoring the existing images of Tang female terracotta figurines using the GLCIC algorithm. It can be seen that the main facial features of the Tang figurines have not been well restored.



(**a**) (**b**) (**c**)

Figure 5. (**a**) Original face image; (**b**) face occlusion image; (**c**) Tang female terracotta figurine face image processed by the original GLCIC algorithm.



(**a**) (**b**) (**c**)

Figure 6. (**a**) Original face image; (**b**) face occlusion image; (**c**) Tang female terracotta figurine face image processed by the original GLCIC algorithm.

3.5.2. Image Inpainting Algorithm for Tang Female Terracotta Figurines

To address the aforementioned issues, we made several improvements to the GLCIC algorithm, mainly in the following aspects:

(1) Given the limited amount of existing Tang female terracotta figurine data, we added a data augmentation module before output. In addition to mirroring and rotation operations, we added Gaussian noise to the images to enhance the robustness of the model training results, considering the varying preservation conditions of Tang figurines. For the mottled, damaged, or feature-missing facial images of Tang female terracotta figurines, we used a guided filter module to smooth the mottled and damaged areas. The Guided Filter is an image-filtering technique proposed by [69]. This filter is particularly suitable for image smoothing while preserving edge information, and is widely used in image enhancement, denoising, and sharpening. Its core idea is to use a guide image (usually the input image itself or another image rich in prior information) to guide the filtering process, ensuring that the output image is smoothed while well-preserving the edges and details of the input image. This is very suitable for the facial images of Tang female terracotta figurines, as the facial features are usually edge information, and the guided filter can remove mottling and damage while protecting the features. The principle of the guided filter is based on a local linear model, which assumes that the output image I' is a local linear transformation of the input image I, For each pixel p, the output $I'(p)$ can be expressed as shown in Equation (2).

$$I'(p) = a(p)I(p) + b(p) \tag{2}$$

Here, $a(p)$ and $b(p)$ are the linear coefficients at pixel p, estimated within a local window W_p centered at p by minimizing the cost function shown in Equation (3).

$$E(a,b) = \sum_{q \in W_p} \left(\left(aI(q) + b - I'(q) \right)^2 + \varepsilon \cdot \left(a^2 + b^2 \right) \right) \tag{3}$$

where q is a pixel in the window W_p, and ε is a regularization parameter to prevent a from becoming too large. The guided filter uses the guide image P to estimate the linear coefficients a and b. The guide image is usually the input image I itself but can also be another image with rich structural information. The guide image P is used to calculate the mean μ_p, variance σ_p^2, and covariance σ_{Ip} of the input image I and the guide image P within the window W_p. By minimizing the cost function $E(a,b)$ concerning a and b, we obtain Equations (4) and (5).

$$a = \frac{\sigma_{Ip} - \mu_p \cdot \mu_{Ip}}{\sigma_p^2 + \varepsilon} \tag{4}$$

$$b = \mu_{Ip} - a \cdot \mu_p \tag{5}$$

where μ_{Ip} is the mean of the input image, I, and the guide image, P, within the window, W_p. Since a and b are estimated based on the statistical properties of the guide image P within the local window, they can adaptively adjust to preserve the edges and details of the image. In edge areas, the variance σ_p^2 of the guide image is larger, resulting in a smaller a, thus reducing the smoothing effect and preserving the edges. Finally, the estimated linear coefficients $a(p)$ and $b(p)$ are applied to the input image I, to obtain the output image I', as shown in Equation (2).

To ensure that the guided filter output image closely approximates the original image, we added a neural network before the guided filter module. This neural network is used to train the regularization parameter ε and the window size W_p. The loss function is a weighted combination of the SSIM and PSNR values of the final output image and the original image, as shown in Equation (6).

$$loss = \alpha \cdot SSIM + \beta \cdot PSNR \tag{6}$$

(2) To address the issue of feature smoothing with the surrounding area after inpainting Tang figurine images, we added an image-sharpening module after the output. This module further sharpens the smoothed feature areas. Since the features in the smoothed areas can be considered edges, we selected the Prewitt gradient operator for enhancement. The specific steps are as follows. 1. Calculate the horizontal and vertical gradients of the image to enhance the edge features. 2. Combine the horizontal and vertical gradients to obtain the edge strength map, further enhancing the details in the image.

The overall architecture of the algorithm is shown in Figure 7, consisting of four main parts: the data augmentation module, the guided filter module, the GLCIC module, and the feature enhancement module.

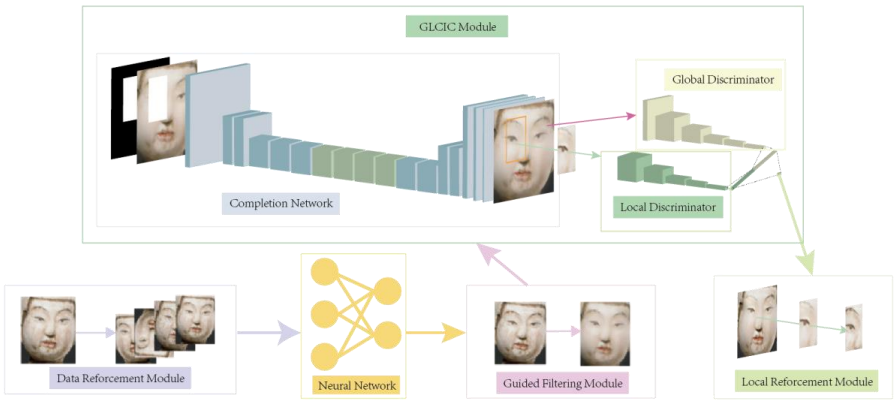


Figure 7. Algorithm architecture diagram.

3.6. Evaluation of the Face Image Inpainting Results

The quality of the images in this study was evaluated from both subjective and objective perspectives. First, we used SSIM and PSNR as objective evaluation tools [70]. PSNR quantified image fidelity by calculating the pixel-level error between the original image and the restored image from a mathematical perspective. SSIM, on the other hand, evaluated the perceived quality of the image based on the human visual system's perception characteristics, considering the structural information of the image. The combined application of these two methods provided a solid quantitative foundation for the comprehensive evaluation of image performance.

Secondly, this study employed the Absolute Category Rating (ACR) as a subjective evaluation method, which is suitable for the subjective assessment of the overall quality of static images [37]. Subjective measurement is the most reliable method to determine the actual image quality, as humans are the ultimate recipients in most applications. We prepared the restored images and ensured they are displayed at the same resolution and on the same monitors. To ensure the broadness and objectivity of the evaluation results, the evaluators of the questionnaire survey were divided into two groups: one group consisted of experts with relevant knowledge and experience, and the other group consisted of students majoring in cultural heritage conservation. Evaluators scored the images based on two aspects: texture and structure, using a discrete five-level scoring scale: Poor (1), Fair (2), Medium (3), Good (4), Excellent (5). Each evaluator scored the images independently, without being influenced by other evaluators. We collected the scores from all evaluators and calculated the average scores and standard deviations for texture and structure. By analyzing the scoring data, we could assess the restoration effectiveness and provide further improvement suggestions based on the evaluators' feedback.

Finally, this study used Pearson correlation analysis to show the degree of correlation between subjective and objective indicators, thereby verifying the consistency and reliability between subjective and objective evaluations. The Pearson correlation coefficient is a common parametric test method used to measure the linear correlation between two

variables [71]. The value of the Pearson correlation coefficient ranges from −1 to +1, where the absolute value closer to 1 indicates a stronger correlation between the variables. The sign of the coefficient indicates the type of correlation: a positive coefficient (positive sign) indicates that when one variable increases, the other variable also increases, whereas a negative coefficient (negative sign) indicates the opposite. The specific values were calculated using SPSS software 29.0.

The aim of this study was to provide a comprehensive evaluation of the restored facial images of the Tang Dynasty terracotta figurines through this diversified evaluation method, providing a scientific and thorough reference for subsequent protection and restoration work.

4. Results and Discussion

4.1. Facial Deficiency Evaluation

Based on expert ratings and FAHP calculations regarding the proportional weights of facial features in Tang Dynasty female terracotta figurines, we used the painted terracotta hand-in-hand standing female figurine from the Palace Museum as an example (Figure 8): the weight for eyes was 0.37, for eyebrows 0.25, for mouth 0.24, and for nose 0.14. The Consistency Index (CI) was 0.09 and the Consistency Ratio (CR) was 0.08. The results indicate that the ranking of the importance of facial features aligns with the conclusions of classical studies [72,73].

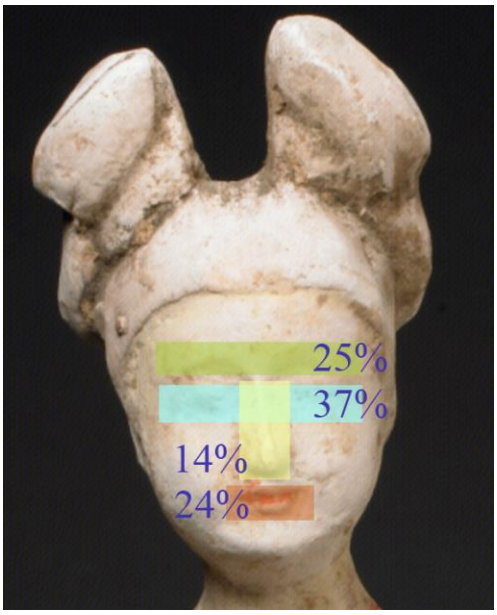


Figure 8. Weight distribution for Tang Dynasty female terracotta figurine facial features.

Regarding facial visual features, the study derives the following weight distribution: shape features account for 0.54 of the overall evaluation, color features account for 0.28, and texture features account for 0.18. The CI was 0.05 and the CR was 0.05. Both consistency ratios are less than 0.1, passing the statistical tests. This indicates that the consistency between indicators has reached an acceptable level of statistical significance.

In evaluating the degree of damage for 491 images of Tang Dynasty female terracotta figurines, this study classified the damage into three levels: slight damage (score range 0–0.4), moderate damage (score range 0.4–0.7), and severe damage (score range 0.7–1). The evaluation results (Figure 9) show that about 9% of the sample images are classified as slightly damaged, approximately 69% as moderately damaged, and 22% as severely damaged.

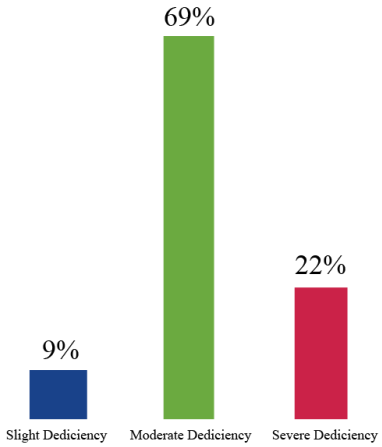


Figure 9. Distribution of facial deficiency degrees in Tang Dynasty terracotta samples.

4.2. Comparison of Face Image Inpainting Algorithms

4.2.1. Evaluation Metrics

The quality of the inpainting results was mainly measured by the structural differences between the restored text images and the original complete images. The human brain can easily distinguish between two images, but this is not easy for computers. Image similarity measurement is not simply obtained through distance calculation. Currently, the Structural Similarity Index Measure (SSIM) and peak signal-to-noise ratio (PSNR) are two commonly used metrics for evaluating image processing results. SSIM is an index that measures the similarity between two images by comparing their brightness, contrast, and structure. The SSIM value ranges from -1 to 1, with 1 indicating that the two images are identical and -1 indicating that they are completely different. PSNR is an objective standard for evaluating images based on the mean squared error, with units in dB. The larger the value, the smaller the distortion.

4.2.2. Results and Analysis

The experimental results are shown in Figures 10–12. Figure 10 shows the face original images, Figure 11 shows the face occlusion images, Figure 12 shows the images processed by the original GLCIC algorithm, and Figure 13 shows the images processed by the improved GLCIC algorithm for Tang Dynasty female terracotta figurines. It can be observed that the results of the improved GLCIC algorithm for Tang Dynasty female terracotta figurines are clearer compared to the original GLCIC algorithm, with a better preservation of the edge information of the facial features. In fact, due to the small sample size, the restoration effect for figurines with significant facial damage was not very good. Currently, this study is more suitable for images with moderate and slight damage.



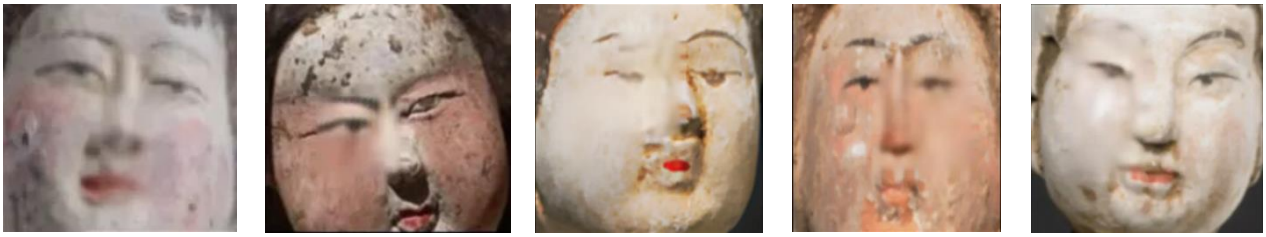
(**a**) (**b**) (**c**) (**d**) (**e**)

Figure 10. Tang Dynasty female terracotta figurine face original images: (**a**) standing female terracotta figurine; (**b**) tricolor female terracotta figurine; (**c**) tricolor standing female terracotta figurine (**d**) Standing female terracotta figurine; (**e**) painted female terracotta figurine.



(**a**) (**b**) (**c**) (**d**) (**e**)

Figure 11. Tang Dynasty female terracotta figurine face occlusion images: (**a**) standing female terracotta figurine; (**b**) tricolor female terracotta figurine; (**c**) tricolor standing female terracotta figurine; (**d**) standing female terracotta figurine; (**e**) painted female terracotta figurine.



(**a**) (**b**) (**c**) (**d**) (**e**)

Figure 12. Tang female terracotta figurine face images processed by the original GLCIC algorithm: (**a**) standing female terracotta figurine; (**b**) tricolor female terracotta figurine; (**c**) tricolor standing female terracotta figurine; (**d**) standing female terracotta figurine; (**e**) painted female terracotta figurine.



(**a**) (**b**) (**c**) (**d**) (**e**)

Figure 13. Tang female terracotta figurine face images processed by the improved GLCIC algorithm for Tang female terracotta figurines: (**a**) standing female terracotta figurine; (**b**) tricolor female terracotta figurine; (**c**) tricolor standing female terracotta figurine; (**d**) standing female terracotta figurine; (**e**) painted female terracotta figurine.

The SSIM and PSNR results of the two algorithms compared to the original images are shown in Table 4. It can be seen that, except for Figure 10d, the SSIM of the images processed by the improved GLCIC algorithm for Tang female terracotta figurines is better than that of the images processed by the original GLCIC algorithm, indicating that the former algorithm is more capable of restoring the facial features of Tang female terracotta figurines. The PSNR of the images processed by both algorithms is roughly the same, indicating that the degree of distortion is mostly consistent. This means that from the perspective of texture and color, the improved algorithm still exhibits issues of texture loss and color blurriness.

A Pearson correlation coefficient analysis of SSIM and PSNR showed a significant positive correlation between these two indicators (PCC = 0.870, significance level $p < 0.05$). This means that in the improved algorithm, a higher SSIM value corresponds to an increase in the PSNR value. In other words, these two objective indicators demonstrated consistent

image quality improvements in the optimized algorithm, indicating that the improved algorithm has consistency and reliability in the overall image quality.

Table 4. SSIM and PSNR of the two algorithms compared to the original images.

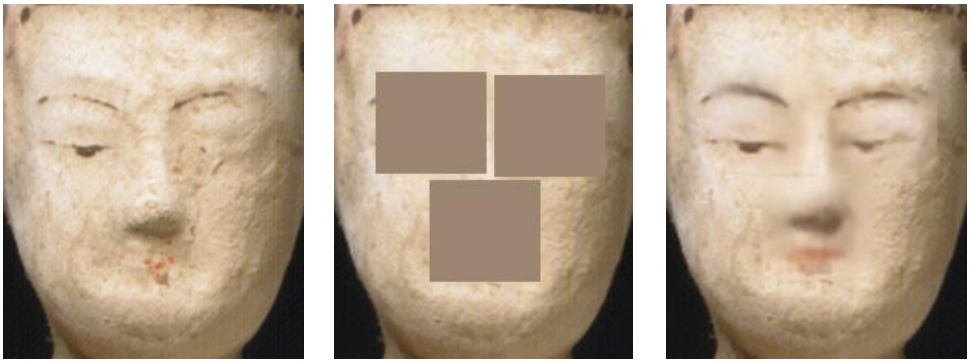
		GLCIC	Improved GLCIC Algorithm for Tang Female Terracotta Figurines
Figure 10a	SSIM	0.6278	0.8698
	PSNR	19.3795	21.3070
Figure 10b	SSIM	0.3785	0.8787
	PSNR	14.0642	27.5678
Figure 10c	SSIM	0.4443	0.8075
	PSNR	15.4271	21.4724
Figure 10d	SSIM	0.6766	0.5536
	PSNR	16.8169	20.5920
Figure 10e	SSIM	0.7435	0.8947
	PSNR	22.4800	25.9771

Regarding the improved GLCIC algorithm for Tang Dynasty female terracotta figurines, although the PSNR value indicates some distortion in the image restoration results, which might affect the clarity of details, the SSIM value suggests good structural similarity in these images. An SSIM value higher than 0.8 indicates that the image restoration performs excellently in maintaining the structure and details of the original image. Therefore, despite the low PSNR value, the overall restoration effect is still good, with the main features and structure of the images being well preserved, and the visual effect remains satisfactory.

4.3. Inpainting and Evaluation of Tang Dynasty Female Terracotta Figurine Facial Images

In this study, to evaluate the generalization ability of the proposed algorithm, we selected a painted terracotta standing female terracotta figurine from the Palace Museum collection as the test object. As shown in Figure 14, the facial features of this standing female terracotta figurine, including the eyes, mouth, and eyebrows, are significantly missing. Based on the previously mentioned calculation of the image damage extent in the study, we can subjectively estimate that the original facial damage extent is 59%, categorized as moderate damage. By applying our algorithm, the generated face image exhibited similarities to the features described in previous studies [32,74], presenting the classical beauty of the female terracotta figurine with delicate eyebrows, slender eyes, and a small cherry-like mouth. In the generated image, the eyebrows and pupils of the female terracotta figurine are painted black, and the mouth is painted red, recreating the typical makeup of Tang Dynasty terracotta figurines. The facial damage extent of the Tang Dynasty female terracotta figurines was reduced to 29% after restoration, categorizing it as slight damage. The restoration results for the significantly damaged facial areas reached a satisfactory level.

Due to the inability to objectively determine the quality of the restoration, this study utilized the ACR method for the subjective evaluation of the restored facial images of Tang Dynasty figurines. A total of 60 questionnaires were collected from cultural heritage students, along with 5 questionnaires from experts in related fields. According to the evaluation results from the cultural heritage students (Table 5), "Shape" received the highest average score among the three evaluation dimensions, indicating that students were generally satisfied with the structural integrity of the restored faces. "Color" followed with an average score of 3.5, reflecting a more neutral evaluation from the students on this dimension. "Texture" received the lowest average score, indicating lower satisfaction with the texture restoration, with a certain proportion of negative evaluations. The standard deviation data show that there was not much divergence in students' opinions across the three dimensions.



(**a**) (**b**) (**c**)

Figure 14. (**a**) Painted terracotta standing female terracotta figurine; (**b**) painted terracotta standing female terracotta figurine occlusion image; (**c**) Tang female terracotta figurine face image processed by the improved GLCIC algorithm for Tang female terracotta figurines.

Table 5. Evaluation results of the students on the restored facial images of Tang Dynasty female terracotta figurines.

Dimension	Shape	Color	Texture
Mean Score	4.0	3.5	2.2
Standard Deviation	0.4	0.61	0.5

The results of the expert questionnaire (Table 6) show that the shape received the highest ratings, with most experts giving it an "excellent" evaluation. The color features followed, with most experts giving it a "medium" evaluation. Finally, texture features received the lowest ratings, which included several "fair" evaluations. The standard deviation data indicate that there was little divergence in the experts' opinions across the three dimensions.

Table 6. Evaluation results of the experts on the restored facial images of Tang Dynasty.

Dimension	Shape	Color	Texture
Mean Score	4.2	3.4	1.8
Standard Deviation	0.4	0.49	0.4

The Pearson correlation coefficient analysis between the two subjective indicators shows a strong positive correlation between the student evaluations and expert evaluations (PCC = 0.997, significance level $p < 0.05$). This indicates that the evaluation results from students and experts are convergent, and the assessment results are reliable.

Overall, the restored images achieved good results in terms of shape features, but there is still room for optimization as they are not yet complete. In terms of color features, although the colors are relatively satisfactory, improvements are needed in aspects such as clarity and saturation. Regarding texture features, the image restoration effect is relatively poor. However, the authenticity of the texture is crucial for the historical value and artistic beauty of the images. Although from the perspective of image restoration, texture is a part that the human visual system can relatively well supplement, enhancing its details remains key. Therefore, future research efforts will focus on further optimizing the restoration algorithms to enhance the overall quality of the restored images from the aspects of shape, color, and texture. This will ensure natural color transitions and precise reproduction of details, thereby more accurately restoring the original appearance of Tang Dynasty terracotta figurines and providing more precise technical support for the protection and display of cultural heritage.

5. Conclusions

This study proposes an improved method based on the GLCIC algorithm to address the issue of facial image inpainting for Tang Dynasty female terracotta figurines. The algorithm introduces data augmentation, guided filtering, and local enhancement modules to effectively solve the problem of unsatisfactory inpainting results when processing small amounts of data with the traditional GLCIC algorithm. The data augmentation module enhanced the robustness and generalization ability of the model by adding Gaussian noise and other techniques. The guided filtering module uses a guide image to protect facial edge information while smoothing the mottled and damaged areas in the image. The local enhancement module sharpened the image using the Prewitt gradient operator, further highlighting the details of facial features.

In analyzing the extent of facial damage in Tang Dynasty female terracotta figurines, we found that approximately 9% of the sample images were evaluated as having minor defects, about 69% were assessed as having moderate defects, and approximately 22% were judged to have severe defects. After applying the improved GLCIC algorithm to restore the faces of these figurines, the experimental results indicated that this algorithm is particularly suitable for images with moderate and minor defects, effectively preserving the edge information and details of facial features.

When objectively evaluating the improved GLCIC algorithm, we observed a significant improvement in SSIM, a critical metric. Specifically, most images had SSIM values exceeding 0.8, approaching 0.9, indicating that the restored images have a high structural similarity to the original images, resulting in more realistic and natural restoration effects. However, in terms of PSNR, despite the improved algorithm achieving PSNR values exceeding 20 dB, there was no significant enhancement, and the values did not reach an ideal state. These results suggest that further optimization of the algorithm is needed in future research to improve the texture details and overall consistency of the restored images.

In the subjective evaluation part of this study, experts and students were invited to assess the quality of images restored using the improved algorithm. The results showed that in the dimension of shape features, the average scores given by both groups exceeded 4, rated as "excellent," reflecting high accuracy in maintaining the original shape features of the restored images. In the color feature dimension, the average scores ranged between 3 and 4, showing a neutral attitude towards the color restoration effect, suggesting that the accuracy of color restoration in terms of hue, saturation, and value may need further optimization. In the texture feature dimension, the average scores were 1.8 for the expert group and 2.2 for the student group, both below the satisfaction threshold, indicating that the restored images did not meet expectations in terms of texture attributes like coarseness and contrast. These findings reveal the limitations of current image restoration technology in texture recovery and highlight the areas requiring attention and improvement in future research.

This study conducted an innovative exploration in the field of facial image restoration for Tang Dynasty female terracotta figurines. There is still room for improvement in shape, color, and texture features, which may be related to factors such as dataset size, model complexity, and algorithm design. In future algorithm improvements, we plan to include more data that capture the shape, color, and texture features of Tang Dynasty female terracotta figurines and enhance the complexity of the algorithms to further improve restoration effects. This study explored new paths and proposed new methods for the protection and preservation of Tang Dynasty female terracotta figurines, expanding the application of facial restoration algorithms in the field of cultural heritage.

Author Contributions: Conceptualization, Q.F. and C.W.; methodology, C.W., S.W. and J.X.; software, S.W.; validation, C.W., S.W. and J.X.; formal analysis, C.W. and J.X.; investigation, Q.F. and C.W.; resources, Q.F. and C.W.; data curation, C.W. and J.X.; writing—original draft preparation, C.W.; writing—review and editing, Q.F.; visualization, C.W.; supervision, Q.F.; project administration, Q.F.; funding acquisition, Q.F. All authors have read and agreed to the published version of the manuscript.

Funding: This research was funded by the Liaoning social science planning fund project, research on scientific identification method of Liao porcelain based on micro-feature analysis, grant number L20BKG001.

Institutional Review Board Statement: Not applicable.

Informed Consent Statement: Not applicable.

Data Availability Statement: The original contributions presented in this study are included in the article. Due to privacy concerns, further inquiries can be directed to the corresponding author.

Conflicts of Interest: The authors declare no conflicts of interest. The funders had no role in the design of the study; in the collection, analyses, or interpretation of data; in the writing of the manuscript; or in the decision to publish the results.

References

1. Wang, Q.; Fan, H.; Zhu, L.; Tang, Y. Deeply Supervised Face Completion with Multi-Context Generative Adversarial Network. *IEEE Signal Process. Lett.* **2019**, *26*, 400–404. [CrossRef]
2. Criminisi, A.; Perez, P.; Toyama, K. Region Filling and Object Removal by Exemplar-Based Image Inpainting. *IEEE Trans. Image Process.* **2004**, *13*, 1200–1212. [CrossRef] [PubMed]
3. Jam, J.; Kendrick, C.; Walker, K.; Drouard, V.; Hsu, J.G.-S.; Yap, M.H. A Comprehensive Review of Past and Present Image Inpainting Methods. *Comput. Vision Image Underst.* **2021**, *203*, 103147. [CrossRef]
4. Qiao, K.; Hou, M.; Lyu, S.; Li, L. Extraction and Restoration of Scratched Murals Based on Hyperspectral Imaging—A Case Study of Murals in the East Wall of the Sixth Grotto of Yungang Grottoes, Datong, China. *Herit. Sci.* **2024**, *12*, 123. [CrossRef]
5. Gao, Z.; Du, M.; Cao, N.; Hou, M.; Wang, W.; Lyu, S. Application of Hyperspectral Imaging Technology to Digitally Protect Murals in the Qutan Temple. *Herit. Sci.* **2023**, *11*, 8. [CrossRef]
6. Yu, K.; Hou, Y.; Fu, Y.; Ni, W.; Zhang, Q.; Wang, J.; Peng, J. Automatic Labeling Framework for Paint Loss Disease of Ancient Murals Based on Hyperspectral Image Classification and Segmentation. *Herit. Sci.* **2024**, *12*, 192. [CrossRef]
7. Nemes, P.; Gordan, M.; Vlaicu, A. Color Restoration in Cultural Heritage Images Using Support Vector Machines. In *Scientific Computing and Cultural Heritage*; Bock, H.G., Jäger, W., Winckler, M.J., Eds.; Contributions in Mathematical and Computational Sciences; Springer: Berlin/Heidelberg, Germany, 2013; Volume 3, pp. 51–59. [CrossRef]
8. Zeng, Y.; Gong, Y. Nearest Neighbor Based Digital Restoration of Damaged Ancient Chinese Paintings. In Proceedings of the 2018 IEEE 23rd International Conference on digital signal processing (DSP), Shanghai, China, 19–21 November 2018; pp. 1–5. [CrossRef]
9. Kumar, K.M.P.; Kumar, M.; Bhargav, B.V.S.; Ghorai, M. Digital Restoration of Deteriorated Mural Images. In Proceedings of the 2014 Fifth International Conference on Signal and Image Processing, Bangalore, India, 8–10 January 2014; pp. 36–41. [CrossRef]
10. Cornelis, B.; Yang, Y.; Vogelstein, J.T.; Dooms, A.; Daubechies, I.; Dunson, D. Bayesian Crack Detection in Ultra High Resolution Multimodal Images of Paintings. In Proceedings of the 2013 18th International Conference on Digital Signal Processing (DSP), Santorini, Greece, 1–3 July 2013; pp. 1–8. [CrossRef]
11. Hu, Q.; Huang, W.; Luo, Y.; Cao, R.; Peng, X.; Peng, J.; Fan, J. Sgrgan: Sketch-Guided Restoration for Traditional Chinese Landscape Paintings. *Herit. Sci.* **2024**, *12*, 163. [CrossRef]
12. Liu, H.; Jiang, B.; Xiao, Y.; Yang, C. Coherent Semantic Attention for Image Inpainting. In Proceedings of the IEEE CVF International Conference on Computer Vision, Seoul, Republic of Korea, 27 October–2 November 2019; pp. 4170–4179.
13. Ren, H.; Sun, K.; Zhao, F.; Zhu, X. Dunhuang Murals Image Restoration Method Based on Generative Adversarial Network. *Herit. Sci.* **2024**, *12*, 39. [CrossRef]
14. Iizuka, S.; Simo-Serra, E.; Ishikawa, H. Globally and Locally Consistent Image Completion. *ACM Trans. Graph.* **2017**, *36*, 1–14. [CrossRef]
15. Pathak, D.; Krahenbuhl, P.; Donahue, J.; Darrell, T.; Efros, A.A. Context Encoders: Feature Learning by Inpainting. In Proceedings of the IEEE Conference on Computer Vision and Pattern Recognition, Las Vegas, NV, USA, 27–30 June 2016; pp. 2536–2544.
16. Yang, C.; Lu, X.; Lin, Z.; Shechtman, E.; Wang, O.; Li, H. High-Resolution Image Inpainting Using Multi-Scale Neural Patch Synthesis. In Proceedings of the IEEE Conference on Computer Vision and Pattern Recognition, Honolulu, HI, USA, 21–26 July 2017; pp. 6721–6729.
17. Cao, J.; Zhang, Z.; Zhao, A.; Cui, H.; Zhang, Q. Ancient Mural Restoration Based on a Modified Generative Adversarial Network. *Herit. Sci.* **2020**, *8*, 7. [CrossRef]
18. Lv, C.; Li, Z.; Shen, Y.; Li, J.; Zheng, J. SeparaFill: Two Generators Connected Mural Image Restoration Based on Generative Adversarial Network with Skip Connect. *Herit. Sci.* **2022**, *10*, 135. [CrossRef]
19. Merizzi, F.; Saillard, P.; Acquier, O.; Morotti, E.; Piccolomini, E.L.; Calatroni, L.; Dessì, R.M. Deep Image Prior Inpainting of Ancient Frescoes in the Mediterranean Alpine Arc. *Herit. Sci.* **2024**, *12*, 41. [CrossRef]
20. Purkait, P.; Ghorai, M.; Samanta, S.; Chanda, B. A Patch-Based Constrained Inpainting for Damaged Mural Images. In *Digital Hampi: Preserving Indian Cultural Heritage*; Mallik, A., Chaudhury, S., Chandru, V., Srinivasan, S., Eds.; Springer: Singapore, 2017; pp. 205–223. [CrossRef]

21. Sun, Z.; Lei, Y.; Wu, X. Ancient Paintings Inpainting Based on Dual Encoders and Contextual Information. *Herit. Sci.* **2024**, *12*, 266. [CrossRef]
22. Adamczak, K.; Osiadacz, M.; Kowalski, Ł.; Szczepańska, G.; Kamiński, D.; Wesołowska, K.; Małecka-Kukawka, J.; Kukawka, S.; Kozicka, M. Digital Restoration and 3D Visualisation of the Early Neolithic Pottery from Ryńsk, Poland. *Digit. Appl. Archaeol. Cult. Herit.* **2024**, *33*, e00337. [CrossRef]
23. Lengauer, S.; Preiner, R.; Sipiran, I.; Karl, S.; Trinkl, E.; Bustos, B.; Schreck, T. Context-Based Surface Pattern Completion of Ancient Pottery. Proceedings of Graphics and Cultural Heritage (GCH), Delft, The Netherlands, 28–30 September 2022; pp. 107–115. [CrossRef]
24. Arbace, L.; Sonnino, E.; Callieri, M.; Dellepiane, M.; Fabbri, M.; Iaccarino Idelson, A.; Scopigno, R. Innovative Uses of 3D Digital Technologies to Assist the Restoration of a Fragmented Terracotta Statue. *J. Cult. Herit.* **2013**, *14*, 332–345. [CrossRef]
25. Sipiran, I.; Mendoza, A.; Apaza, A.; Lopez, C. Data-Driven Restoration of Digital Archaeological Pottery with Point Cloud Analysis. *Int. J. Comput. Vis.* **2022**, *130*, 2149–2165. [CrossRef]
26. Zhou, Z. Appreciation of the Artistic Modeling of Tang Sancai under the Splendor of the Tang Dynasty. *High. Corresp. J. (Nat. Sci. Ed.)* **2006**, *8*, 150–152.
27. Chen, X. *The Culture of Ancient Chinese Sculpture*, 1st ed.; Nanjing University Press: Nanjing, China, 2021.
28. Chen, W.; Fan, M. *Grand Tang: A Study of Tang Dynasty Aesthetic Consciousness*; Jiangsu People's Publishing House: Nanjing, China, 2022; p. 327.
29. Yu, F.; Zhang, J. An Overview of Tang Sancai. *Cent. Plains Cult. Relics* **1994**, *100*, 61–64.
30. Ma, X. Changes in the Themes and Aesthetic Styles of Tang Figurines. *Meiyuan* **1994**, 65–71.
31. Li, F. Exploration of the Unique Aesthetic Characteristics of the Tang Dynasty through Tang Sancai. *Chin. Ceram.* **2009**, *45*, 74–76. [CrossRef]
32. Guo, K. On the Transcendence of Tang Sancai over Traditional Chinese Modeling Patterns. *J. Zhengzhou Univ. (Philos. Soc. Sci. Ed.)* **2004**, *37*, 148–150.
33. Han, C.; Tian, Y.; Shang, C.; Zhang, X.; Zhang, M.; Cui, H. A Brief Report on the Excavation of Tang Dynasty Tombs at Hanzhang Village, Mengzhou, Jiaozuo. *Cent. Plains Cult. Relics* **2024**, *145*, 25–33.
34. Sun, J. Review of Archaeological Discoveries and Research on Gongyi Kiln. *Central Plains Cultural Relics* **2024**, *No. 4*, 107–114.
35. Rudin, L.I.; Osher, S.; Fatemi, E. Nonlinear Total Variation Based Noise Removal Algorithms. *Phys. D Nonlinear Phenom.* **1992**, *60*, 259–268. [CrossRef]
36. Efros, A.A.; Leung, T.K. Texture Synthesis by Non-Parametric Sampling. In Proceedings of the Seventh IEEE International Conference on Computer Vision, Corfu, Greece, 20–25 September 1999; Volume 2, pp. 1033–1038. [CrossRef]
37. Liu, T.-J. Study of Visual Quality Assessment on Pattern Images: Subjective Evaluation and Visual Saliency Effects. *IEEE Access* **2018**, *6*, 61432–61444. [CrossRef]
38. Lyu, Q.; Zhao, N.; Yang, Y.; Gong, Y.; Gao, J. A Diffusion Probabilistic Model for Traditional Chinese Landscape Painting Super-Resolution. *Herit. Sci.* **2024**, *12*, 4. [CrossRef]
39. Tang, H.; Geng, G.; Zhou, M. Application of Digital Processing in Relic Image Restoration Design. *Sens. Imaging* **2019**, *21*, 6. [CrossRef]
40. Sun, X.; Jia, J.; Xu, P.; Ni, J.; Shi, W.; Li, B. Structure-Guided Virtual Restoration for Defective Silk Cultural Relics. *J. Cult. Herit.* **2023**, *62*, 78–89. [CrossRef]
41. Aharon, M.; Elad, M.; Bruckstein, A. K-SVD: An Algorithm for Designing Overcomplete Dictionaries for Sparse Representation. *IEEE Trans. Signal Process.* **2006**, *54*, 4311–4322. [CrossRef]
42. Yu, J.; Lin, Z.; Yang, J.; Shen, X.; Lu, X.; Huang, T.S. Generative Image Inpainting with Contextual Attention. In Proceedings of the 2018 IEEE/CVF Conference on Computer Vision and Pattern Recognition, Salt Lake City, UT, USA, 18–23 June 2018; pp. 5505–5514. [CrossRef]
43. Hedjam, R.; Cheriet, M. Historical Document Image Restoration Using Multispectral Imaging System. *Pattern Recognit.* **2013**, *46*, 2297–2312. [CrossRef]
44. Wang, H.; Li, Q.; Jia, S. A Global and Local Feature Weighted Method for Ancient Murals Inpainting. *Int. J. Mach. Learn. Cyber.* **2020**, *11*, 1197–1216. [CrossRef]
45. Chen, M.; Liu, Z.; Ye, L.; Wang, Y. Attentional Coarse-and-Fine Generative Adversarial Networks for Image Inpainting. *Neurocomputing* **2020**, *405*, 259–269. [CrossRef]
46. Zou, Z.; Zhao, P.; Zhao, X. Virtual Restoration of the Colored Paintings on Weathered Beams in the Forbidden City Using Multiple Deep Learning Algorithms. *Adv. Eng. Inf.* **2021**, *50*, 101421. [CrossRef]
47. Li, Z.; Zhang, Y.; Du, Y.; Wang, X.; Wen, C.; Zhang, Y.; Geng, G.; Jia, F. STNet: Structure and Texture-Guided Network for Image Inpainting. *Pattern Recognit.* **2024**, *156*, 110786. [CrossRef]
48. Xiang, H.; Zou, Q.; Nawaz, M.A.; Huang, X.; Zhang, F.; Yu, H. Deep Learning for Image Inpainting: A Survey. *Pattern Recognit.* **2023**, *134*, 109046. [CrossRef]
49. Barnes, C.; Shechtman, E.; Finkelstein, A.; Goldman, D.B. PatchMatch: A Randomized Correspondence Algorithm for Structural Image Editing. *ACM Trans. Graph.* **2009**, *28*, 24. [CrossRef]
50. Darabi, S.; Shechtman, E.; Barnes, C.; Goldman, D.B.; Sen, P. Image Melding: Combining Inconsistent Images Using Patch-Based Synthesis. *ACM Trans. Graph.* **2012**, *31*, 1–10. [CrossRef]

51. Corneanu, C.; Gadde, R.; Martinez, A.M. Latentpaint: Image Inpainting in Latent Space with Diffusion Models. In Proceedings of the IEEE/CVF Winter Conference on Applications of Computer Vision, Waikoloa, HI, USA, 3–8 January 2024; pp. 4334–4343.
52. Deng, Q.; Cao, J.; Liu, Y.; Li, Q.; Sun, Z. R-FACE: Reference Guided Face Component Editing. *Pattern Recognit.* **2024**, *152*, 110425. [CrossRef]
53. Zhang, X.; Wang, X.; Shi, C.; Yan, Z.; Li, X.; Kong, B.; Lyu, S.; Zhu, B.; Lv, J.; Yin, Y.; et al. DE-GAN: Domain Embedded GAN for High Quality Face Image Inpainting. *Pattern Recognit.* **2022**, *124*, 108415. [CrossRef]
54. Shen, Z.; Lai, W.-S.; Xu, T.; Kautz, J.; Yang, M.-H. Deep Semantic Face Deblurring. In Proceedings of the IEEE Conference on Computer Vision and Pattern Recognition, Salt Lake City, UT, USA, 18–23 June 2018; pp. 8260–8269.
55. Bulat, A.; Tzimiropoulos, G. Super-Fan: Integrated Facial Landmark Localization and Super-Resolution of Real-World Low Resolution Faces in Arbitrary Poses with Gans. In Proceedings of the IEEE Conference on Computer Vision and Pattern Recognition, Salt Lake City, UT, USA, 18–23 June 2018; pp. 109–117.
56. Grm, K.; Scheirer, W.J.; Štruc, V. Face Hallucination Using Cascaded Super-Resolution and Identity Priors. *IEEE Trans. Image Process.* **2019**, *29*, 2150–2165. [CrossRef]
57. Deng, J.; Cheng, S.; Xue, N.; Zhou, Y.; Zafeiriou, S. UV-GAN: Adversarial Facial UV Map Completion for Pose-Invariant Face Recognition. In Proceedings of the IEEE Conference on Computer Vision and Pattern Recognition, Salt Lake City, UT, USA, 18–23 June 2018; pp. 7093–7102.
58. Ren, W.; Yang, J.; Deng, S.; Wipf, D.; Cao, X.; Tong, X. Face Video Deblurring Using 3D Facial Priors. In Proceedings of the IEEE/CVF International Conference on Computer Vision, Seoul, Republic of Korea, 27 October–2 November 2019; pp. 9388–9397.
59. Wan, Z.; Zhang, B.; Chen, D.; Zhang, P.; Wen, F.; Liao, J. Old Photo Restoration via Deep Latent Space Translation. *IEEE Trans. Pattern Anal. Mach. Intell.* **2022**, *45*, 2071–2087. [CrossRef] [PubMed]
60. Mikhailov, L. A Fuzzy Programming Method for Deriving Priorities in the Analytic Hierarchy Process. *J. Oper. Res. Soc.* **2000**, *51*, 341–349. [CrossRef]
61. Zadeh, L.A. Fuzzy Sets. *Inf. Control* **1965**, *8*, 338–353. [CrossRef]
62. Deng, H. Multicriteria Analysis with Fuzzy Pairwise Comparison. *Int. J. Approx. Reason.* **1999**, *21*, 215–231. [CrossRef]
63. Kahraman, C.; Cebeci, U.; Ruan, D. Multi-Attribute Comparison of Catering Service Companies Using Fuzzy AHP: The Case of Turkey. *Int. J. Prod. Econ.* **2004**, *87*, 171–184. [CrossRef]
64. Guo, A.; He, P.; Min, Q.; Xu, S. A Fuzzy Comprehensive Evaluation Method for Assessing the Damage Degree of Cultural Relics Based on an Improved AHP-EWM Coupled Weight Model and a Modified Ridge Function. *Herit. Sci.* **2024**, *12*, 378. [CrossRef]
65. Cakir, O.; Canbolat, M.S. A Web-Based Decision Support System for Multi-Criteria Inventory Classification Using Fuzzy AHP Methodology. *Expert Syst. Appl.* **2008**, *35*, 1367–1378. [CrossRef]
66. Karczmarek, P.; Pedrycz, W.; Kiersztyn, A.; Rutka, P. A Study in Facial Features Saliency in Face Recognition: An Analytic Hierarchy Process Approach. *Soft Comput.* **2017**, *21*, 7503–7517. [CrossRef]
67. Ping Tian, D. A Review on Image Feature Extraction and Representation Techniques. *Int. J. Multimed. Ubiquitous Eng.* **2013**, *8*, 385–396.
68. Tamura, H.; Mori, S.; Yamawaki, T. Textural Features Corresponding to Visual Perception. *IEEE Trans. Syst. Man Cybern.* **1978**, *8*, 460–473. [CrossRef]
69. He, K.; Sun, J.; Tang, X. Guided Image Filtering. *IEEE Trans. Pattern Anal. Mach. Intell.* **2013**, *35*, 1397–1409. [CrossRef] [PubMed]
70. Horé, A.; Ziou, D. Image Quality Metrics: PSNR vs. SSIM. In Proceedings of the 2010 20th International Conference on Pattern Recognition, Istanbul, Turkey, 23–26 August 2010; pp. 2366–2369. [CrossRef]
71. Asuero, A.G.; Sayago, A.; González, A.G. The Correlation Coefficient: An Overview. *Crit. Rev. Anal. Chem.* **2006**, *36*, 41–59. [CrossRef]
72. Haig, N.D. Exploring Recognition with Interchanged Facial Features. *Perception* **1986**, *15*, 235–247. [CrossRef] [PubMed]
73. Davies, G.; Ellis, H.; Shepherd, J. Cue Saliency in Faces as Assessed by the 'Photofit' Technique. *Perception* **1977**, *6*, 263–269. [CrossRef]
74. Zhou, H. Research on the Art of Tang Sancai. *Art Crit.* **2013**, *29* (Suppl. S1), 227–228.

Disclaimer/Publisher's Note: The statements, opinions and data contained in all publications are solely those of the individual author(s) and contributor(s) and not of MDPI and/or the editor(s). MDPI and/or the editor(s) disclaim responsibility for any injury to people or property resulting from any ideas, methods, instructions or products referred to in the content.